Ion Fragment Imaging of the Photodissociation of Methyl Iodide Small Clusters at 266 nm

Yoshiki Tanaka, Masahiro Kawasaki,* and Yutaka Matsumi†

Department of Molecular Engineering, Kyoto University, Kyoto 606-8501

†Solar Terrestrial Environment Laboratory, Nagoya University, Toyokawa 442-8507

(Received April 24, 1998)

Photofragment iodine atoms and methyl radicals from the photodissociation of small clusters of methyl iodide at 266 nm were detected, using ion photofragment imaging spectroscopy. Three different components of the I^+ image were observed with average laboratory translational energies of the I fragments, $\langle E(I)\rangle$ = 2, 16, and 25 kcal## mol^{-1} and anisotropy parameters, β = 0, 2.0±0.6, and 2.1±0.5, respectively. Similarly, for CH_3^+ three different components in the CH_3^+ image correspond to average laboratory translational energies, $\langle E(CH_3)\rangle$ = 5, 25, and 38 kcal mol^{-1} and β = 0, 2.0±0.2, and 2.2±0.6, respectively. These results suggest the following reaction mechanisms; a) a CH_3I chromophore in small clusters is excited to the A band (n,σ^*) system of free CH_3I, survives intact within the clusters and dissociates, b) dissociation of the CH_3I moiety in the small clusters that have two adjacent iodine atoms results in the formation of slow photofragment iodine atoms and fast methyl radicals, and c) dissociation of other types of small clusters results in the formation of fast iodine atoms and slow methyl radicals.

The UV photodissociation of CH_3I from the A band (n,σ^*) absorption has been studied extensively both theoretically[1] and experimentally.[2] Dissociation is prompt (0.15 ps) with a highly anisotropic angular distribution of the fragments, CH_3 and $I(^2P_{1/2})$ as major products, and CH_3 and $I(^2P_{3/2})$ as minor ones,

$$CH_3I + h\nu \longrightarrow CH_3 + I(^2P_{1/2}), \quad (1)$$

$$\longrightarrow CH_3 + I(^2P_{3/2}). \quad (2)$$

Under supersonic expansion conditions, dimers and higher clusters of CH_3I molecules are formed in a molecular beam.[3] Semiempirical calculations predict a bent head-to-head ground-state equilibrium structure for the dimer. The I–I distance is 3.0 Å, and the C–I···I–C angles are 170° and 115°.[4] The dissociation energy of the dimer is estimated to be about 500 cm^{-1}.[5] When dimers of CH_3I are irradiated in the ultraviolet, I atoms are produced through the following reaction sequence, according to Zhong et al.[2]

$$CH_3I\cdots ICH_3 + h\nu \longrightarrow [CH_3I + I] + CH_3, \quad (3)$$

$$[CH_3I + I] \longrightarrow [CH_3I\text{–}I]^{\#}, \quad (4)$$

$$[CH_3I\text{–}I]^{\#} \longrightarrow CH_3I + I, \quad (5)$$

where $[\cdots]^{\#}$ stands for a collision complex. In Reaction 3, an iodine atom is formed in 0.15 ps by detaching the CH_3 group in direct photodissociation of the CH_3I moiety. Zhong et al.[2] monitored I atom production in real time from the vibrationally excited collision complex $[CH_3I\text{–}I]^{\#}$. They reported a delay time of 1.4 ps for Reaction 4 and a rise time of 1.7 ps for Reaction 5. The long-lived complex, $[CH_3I\text{–}I]^{\#}$, produced by the intra-cluster collision process yields an I atom that has a broad angular distribution. Syage[6] observed Doppler profiles for recoil of I atoms produced from dimers. The Doppler profile consists mostly of a slow isotropic component with a small portion of a fast anisotropic component. The slow component is consistent with a long-lived complex mechanism, while the source of the fast one is unclear. Direct detection of the partner photofragment, CH_3, is essential to discover the detailed mechanism of these reactions.

In addition to the I production, Fan et al.[7] reported that I_2 molecules in the ground state that have very little internal energy are produced through cooperative nuclear motion of both C–I bonds in the four-center reaction,

$$CH_3I\cdots ICH_3 + h\nu \longrightarrow CH_3\cdots I\text{–}I\cdots CH_3 \longrightarrow CH_3 + I_2 + CH_3. \quad (6)$$

It was proposed by Syage[6] that the origin of the fast anisotropic I atom from the dimer could be secondary photodissociation of this I_2 molecule, but this interpretation is uncertain. In this work, we have measured the translational energy and angular distributions of I and CH_3 from the photodissociation of small clusters of CH_3I at 266 nm with photofragment imaging spectroscopy.

Experimental

The experimental apparatus design is similar to that reported by Chandler and Houston[8] and was described in detail elsewhere.[9] In brief, the three axes of the molecular beam, laser beam, and time-

1 cal = 4.184 J.

of-flight mass spectrometer are mutually orthogonal in the interaction region. To produce a supersonic molecular beam, a pulsed valve, a skimmer, and a collimator are used. The 266-nm laser beam, which is used for both photodissociation of molecules and ionization of CH_3 and I photofragments, is the 4th harmonic of a YAG laser light (Spectra Physics, DCR-11, 5 mJ/pulse, 10 Hz) and is focused with a lens (f = 200 mm) into the molecular beam. This one-color laser scheme was previously reported by Danon et al.[10] The generated ions are accelerated to the detector chamber with grid electrodes of nickel etched mesh. The acceleration voltage is 2 and 4 kV for I^+ and CH_3^+ ion, respectively. A CCD camera attached to a gated image intensifier monitors the ion images on a phosphor screen. The image signal from the camera is accumulated by a microcomputer over 10000 laser pulses. The resulting two-dimensional images have a striped shadow due to trajectory deflections caused by the grid electrodes. Hence, the two-dimensional images are first filtered in the frequency domain to eliminate the striped shadow. To recover a three-dimensional velocity distribution from a two-dimensional image, the filtered back-projection procedure is used.[11] Equatorial slices of the three-dimensional distributions are obtained to find the translational energy and angular distributions of the photofragments. Note that the image radius actually scales linearly with velocity, so that the energy resolution should be energy-dependent. Thus, for example, for the Cl fragment with fragment translational energy of 20 kcal mol^{-1}, the full-width-at-half-maximum energy resolution is about 6.5 kcal mol^{-1}.

Sample gases, typically 5% diluted in Ar (total 9.3×10^4 Pa) for monomer experiments and neat (4.0×10^4 Pa) for cluster experiments are expanded in the supersonic molecular beam condition. For both the monomer and cluster experiments, the delay time between the molecular beam and YAG laser pulse is set typically at 0.2 ms. To measure size distribution of the clusters in the molecular beam of neat methyl iodide, time-of-flight mass spectra are measured by irradiating the molecular beam with a focused UV laser at 207 nm (0.5 mJ/pulse) with a dye laser (Lambda Physik, ScanMate).

Results

A. Photodissociation of CH_3I Monomers at 266 nm. Figure 1 shows the experimentally obtained two-dimensional images. For monomer photodissociation, the molecular beam of 5% CH_3I diluted in Ar was irradiated at 266 nm. The upper half panel of Fig. 1 shows sharp two-ring images of CH_3^+ and a small diffuse ring image of I^+. We assume a one-color laser scheme for one-photon dissociation of CH_3I accompanied by multiphoton ionization of the photofragments at 266 nm.[10] Since the CH_3^+ images are essentially the same as those reported by Chandler et al.,[12] the inner and outer rings of the CH_3^+ images correspond to formation of $I(^2P_{1/2})$ and $I(^2P_{3/2})$, respectively.

$$CH_3I + h\nu\ (266\ \text{nm}) \longrightarrow CH_3 + I(^2P_{1/2})/I(^2P_{3/2}), \quad (7)$$

$$CH_3 + 3h\nu \longrightarrow CH_3^+, \quad (8)$$

$$I(^2P_{1/2}) + 2h\nu \longrightarrow I^+, \quad (9)$$

$$I(^2P_{3/2}) + 3h\nu \longrightarrow I^+. \quad (10)$$

After backprojection of the image, the speed distribution is obtained from the radial distribution, and then converted to the distribution of center-of-mass (c.m.) translational energy. The upper panel of Fig. 2 shows the c.m. translational energy distribution from the ring images of CH_3^+. The inset shows the energy distribution reported by Sparks et al.[13] Although our ion imaging apparatus does not have the energy resolution of the best of molecular beam machines, the gross features of the distributions are the same; that is, the major process is $CH_3+I(^2P_{1/2})$ and the minor one is $CH_3+I(^2P_{3/2})$. A small contribution from the dissociation of clusters in the molecular beam is also seen as a Maxwell–Boltzmann distribution. Similarly, the diffuse ring of I^+ from the photofragments $I(^2P_{3/2})$ and $I(^2P_{1/2})$ is analyzed. The upper panel of Fig. 3 shows the fragment translational energy of the I atoms. The main feature of the c.m. translational energy distribution is in agreement with Reaction 1, or $CH_3+I(^2P_{1/2})$.

The angular distributions $I(\theta)$ for the inner and outer rings of the CH_3^+ images are fitted with $\beta = 2.1\pm0.2$ and 2.0 ± 0.1, respectively,

$$I(\theta) = (1/4\pi)\{1 + \beta P_2(\cos\theta)\}, \quad (11)$$

where β is the angular anisotropy parameter, $P_2(x)$ is the second Legendre polynomial, and θ is the angle between the laser polarization and the recoil vector.[14] Our anisotropy parameters for CH_3 are in good agreement with the values (1.8—1.9) reported earlier for the 266 nm photodissociation of CH_3I.[2,15—17]

B. Photodissociation of Small Clusters at 266 nm. CH_3I clusters were formed under our molecular beam conditions with a backing pressure of 4×10^4 Pa for neat methyl iodide. Figure 4 is a typical time-of-flight mass spectrum when the molecular beam was irradiated at 207 nm near the Rydberg transition of free CH_3I. A range of $(CH_3I)_n$ cluster sizes is expected in the molecular beam expansion, but only I^+ and I_2^+ were seen in the spectrum along with weak CH_3^+ and CH_3I^+ signals. The relative ratio of I_2^+/I^+ increased with the delay time between the molecular beam and UV laser pulse. These ions come from dissociative ionization of monomer and clusters. The I_2^+ formation is consistent with the I_2 formation from the dimer photodissociation reported by Fan et al.[7] as shown in Reaction 6. If small clusters have two adjacent iodine atoms, I–I, then I_2^+ is easily produced by the strong VUV laser pulses. These results suggest that a substantial fraction of the molecules are in the form of dimers, with a small fraction of larger clusters.[3]

When the molecular beam of the clusters were excited at 266 nm, photofragment CH_3 radicals and I atoms were produced and ionized via a one-color laser scheme at 266 nm:

$$(CH_3I)_n + h\nu \longrightarrow (CH_3I)_{n-1} + CH_3 + I, \quad (12)$$

$$CH_3/I + mh\nu \longrightarrow CH_3^+/I^+. \quad (13)$$

Images of CH_3^+. The lower left panel of Fig. 1 shows the image of CH_3^+ when the molecular beam of neat methyl iodide was irradiated at 266 nm. The CH_3^+ image is essentially the same as that observed from the monomer photodissociation. Assuming dissociation of a C–I bond in the dimer through Reaction 3 producing a partner fragment

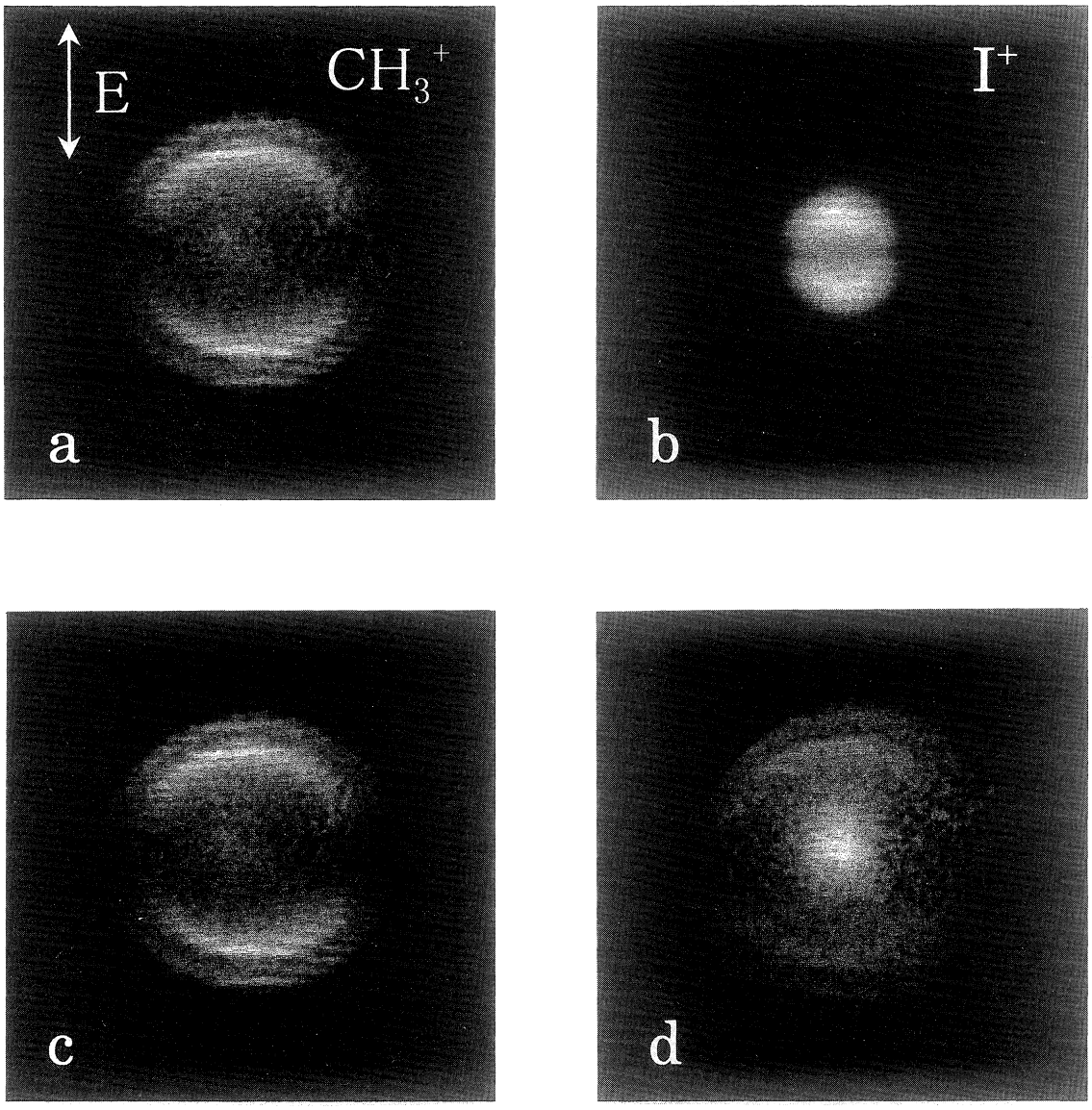

Fig. 1. Two-dimensional images of CH_3^+ and I^+ from the 266 nm photodissociation of supersonic molecular beams of 5% CH_3I diluted with Ar at a total pressure of 9.3×10^4 Pa (upper panel a and b) and neat CH_3I at a pressure of 4.0×10^4 Pa (lower panel c and d). The scale of the I^+ figures is enlarged by 1.4 for clarity. The electric vector of the dissociation laser light lies in the plane, as shown by the arrow.

of CH_3I–I, the c.m. translational energy distributions for the sharp ring images may be calculated to give $\langle E_t \rangle = 28$ and 42 kcal mol^{-1}, as shown in the lower panel of Fig. 2. Even if higher clusters are photodissociated, the c.m. energy distribution is shifted toward the lower energy side, at most, by 10%, because the mass of CH_3 is much smaller than that of CH_3I. As shown in Fig. 5, the angular distributions for the inner and outer rings are fitted with $\beta = 2.0\pm0.2$ and 2.2 ± 0.6, respectively. Because the energy and angular distributions are quite similar to those for the monomer dissociation, the dissociation dynamics for production of CH_3 from a small cluster must be the same as for a free CH_3I in the valence excited state, that is, a major process is the photodissociation to $CH_3+I(^2P_{1/2})$, and a minor one is to $CH_3+I(^2P_{3/2})$.

Since methyl iodide monomers exist in the molecular beam, some contribution of the monomer photodissociation to this CH_3^+ image is indistinguishable. However, as will be shown below, the corresponding image of I^+ is totally different from that of monomer photodissociation. It is reasonable to assume that the CH_3^+ image of Fig. 1 (lower left) comes mostly from the cluster photodissociation.

Images of I^+. Three different images of I^+ are shown in the lower right panel of Fig. 1. The central image has a major contribution, while the sharp ring images have a minor contribution. These experimental conditions favor cluster formation, as shown by the isotropic central feature of the I^+ image. These images for I atoms originating from the small clusters are dissimilar to those from a free CH_3I shown in the upper right panel of Fig. 1. The observed images are transformed into a fragment translational energy frame, as shown in the lower panel of Fig. 3. Note that this is not a c.m. energy frame. The obtained distribution is best fitted with the sum of three different functions, a Maxwell–Boltzmann and two Gaussian functions, which have average translational

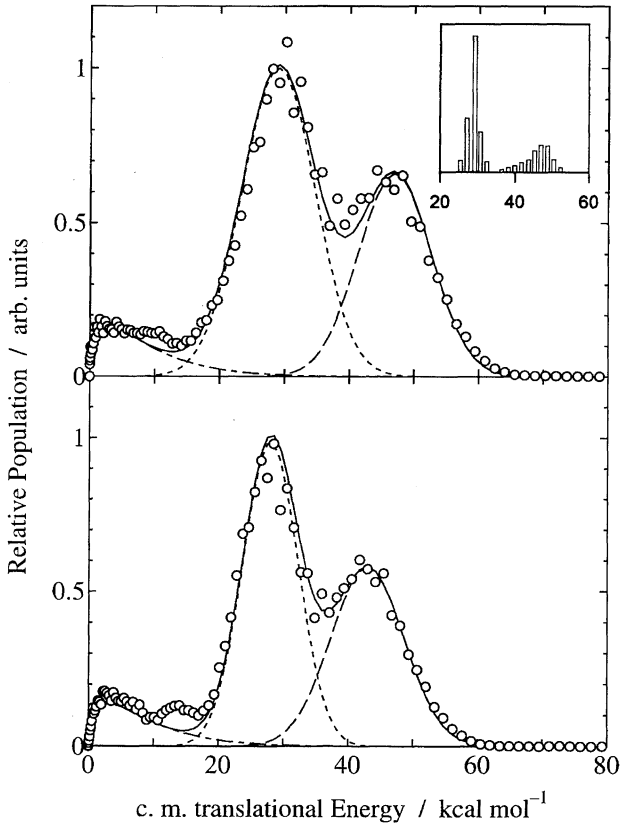

Fig. 2. Center-of-mass translational energy distributions calculated from the CH_3^+ images for monomer dissociation (upper panel) and clusters (lower panel). For the lower panel, the dimer dissociation mechanism is assumed in the calculation of the c.m. translational energy. The inset for the monomer photodissociation at 266 nm is taken from Sparks et al. (Ref. 13).

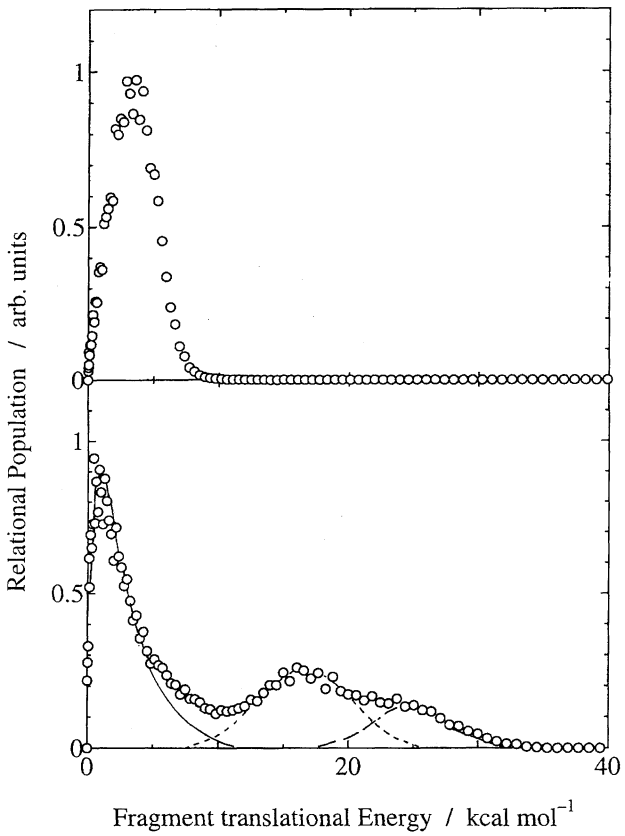

Fig. 3. Fragment translational energy distributions of I atoms calculated from the I^+ images for monomer dissociation (upper panel) and clusters (lower panel). The lower curve is fitted with a sum of a low-energy Maxwell–Boltzmann (M–B) distribution and two high-energy Gaussian distributions. Note that the upper curve does not match the M–B component of the lower panel.

energies of the I fragments, $\langle E(\mathrm{I})\rangle = 2$, 16, and 25 kcal mol^{-1}, respectively. For the bimodal ring images with $\langle E(\mathrm{I})\rangle = 16$ and 25 kcal mol^{-1}, the relative intensity ratio is 3 to 1, and the angular distributions shown in Fig. 6 are best-fitted with $\beta = 2.0\pm0.6$ and 2.1 ± 0.5, respectively.

Production of fast I atoms from the UV photodissociation of small clusters of CH_3I and HI were reported by Syage[6] and Young,[18] respectively. Observing Doppler profiles of I atoms from cluster photodissociation of CH_3I at 266 nm, Syage[6] analyzed the Doppler profiles with a Maxwell–Boltzmann energy distribution and velocity-dependent anisotropy parameters, β. The parameters ranged from zero at $v = 0$ to 1 at $v = 1$ km s^{-1} or $E(\mathrm{I}) = 15$ kcal mol^{-1}. In their experiment, the main feature was from slow I atoms with an isotropic angular distribution and a minor feature from fast I atoms with high anisotropy. In our experiment, the velocity components are clearly resolved, with one isotropic central image and two anisotropic ring images.

Discussion

A. Formation Mechanism of CH_3^+ and I^+ from Multiphoton Processes for Monomer CH_3I. As indicated above, these results for formation of CH_3^+ and I^+ from the photodissociation of CH_3I are reasonably explained, assuming one-photon dissociation of CH_3I at 266 nm followed by multiphoton ionization of the photofragment CH_3 and I via Reactions 7—10. Danon et al.[10] suggested this path in their multiphoton excitation study for CH_3I. The two-photon tran-

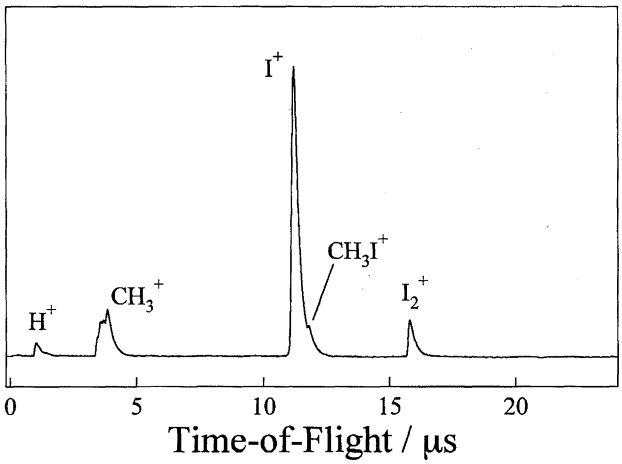

Fig. 4. Time-of-flight mass spectrum of ions observed when the molecular beam of neat CH_3I (4.0×10^4 Pa) was irradiated by focused laser light at 207 nm.

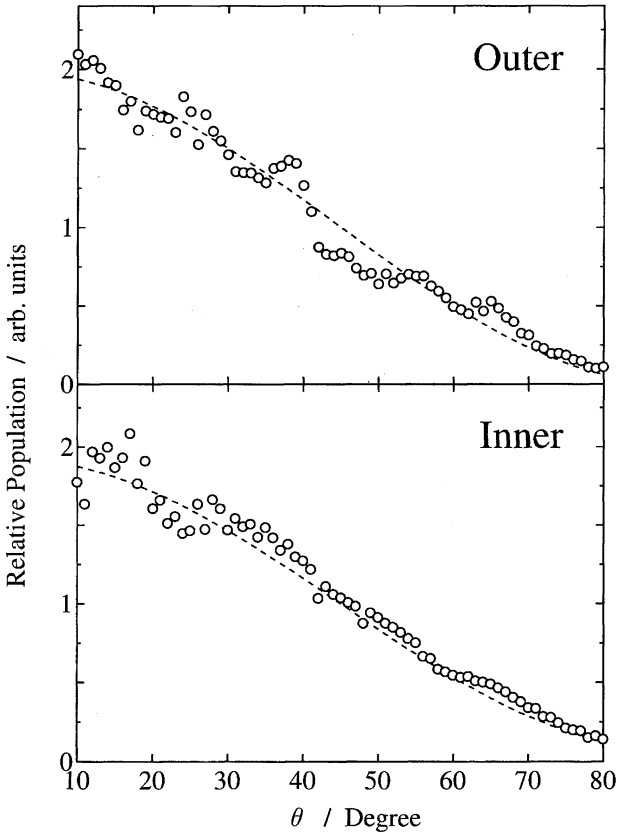

Fig. 5. Angular distributions of CH_3 photofragments produced from the photodissociation of clusters at 266 nm. Upper and lower panels are for the outer and inner ring images of Fig. 1(c), respectively. Solid curves are angular distbributions calculated from Eq. 11 with $\beta = 2.2$ (upper) and 2.0 (lower).

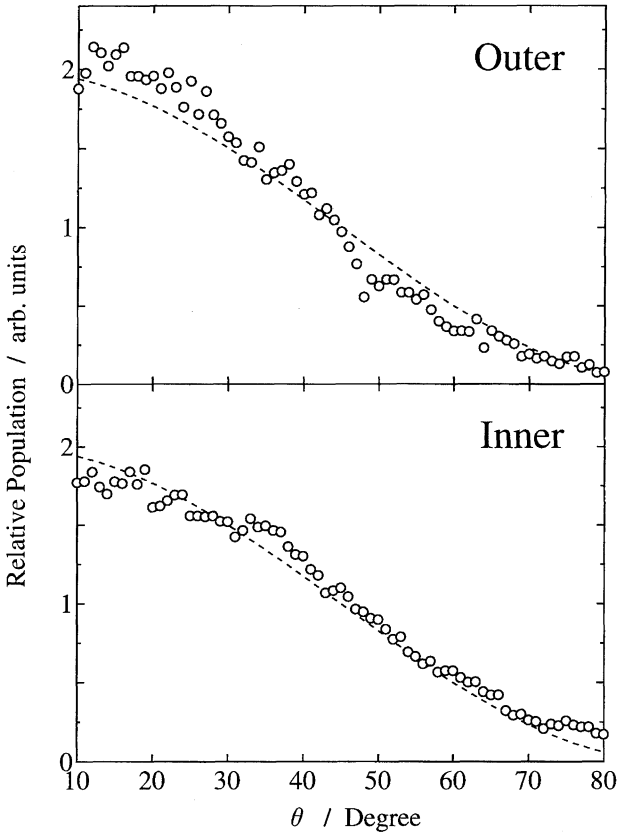

Fig. 6. Angular distributions of I atoms produced from the photodissociation of clusters at 266 nm. Upper and lower panels are for the outer and inner ring images of Fig. 1(d), respectively. Solid curves are angular distributions calculated from Eq. 11 with $\beta = 2.1$ (upper) and 2.0 (lower).

sition of $CH_3(^2E'(5f) \leftarrow X^2A')$ is involved in its multiphoton ionization at 266 nm.[19] For I atoms a moderate ionization cross section was reported by Lubman et al.,[20] because, near 266 nm, the two-photon resonant states for (2+1) resonant ionization exist at 266.4, 265.9, and 266.5 nm.[21]

Another possible reaction mechanism for formation of CH_3^+ and I^+ ions is one-photon dissociation of CH_3I^+ after three-photon absorption of the parent molecules.

$$CH_3I + 3h\nu\ (266\ \text{nm}) \longrightarrow CH_3I^+(X^2E_{1/2})/CH_3I^+(^2E_{3/2}) \quad (14)$$

$$CH_3I^+(X^2E_{1/2})/CH_3I^+(^2E_{3/2}) + h\nu \longrightarrow CH_3I^+(A^2E_{1/2})/CH_3I^+(B^2E_{3/2}) \quad (15)$$

$$CH_3I^+(A^2E_{1/2})/CH_3I^+(B^2E_{3/2}) \longrightarrow CH_3^+ + I(^2P_{1/2})/I(^2P_{3/2}) \quad (16)$$

$$\longrightarrow CH_3 + I^+. \quad (17)$$

Photofragmentation of $CH_3I^+(A^2E_{1/2}$ and $B^2E_{3/2})$ to produce CH_3^+ was investigated at 335—403 nm by Kawasaki et al.[22] They reported that in this wavelength range predissociation occurs through vibrationally excited ground state ions, with $\beta = 0$ for the B state and 0.11—0.67 for the A state. Eland[23] estimated that the internal conversion rate of CH_3I^+ from the B state to the A state is fast. For 266 nm photoexcitation, both $CH_3I^+(X^2E_{1/2}$ and $X^2E_{3/2})$ are excited to $CH_3I^+(B^2E_{3/2})$ and predissociates to form CH_3^+. If so, the β value is expected to be low due to a) the slow dissociation rate, b) possible mixing of two (or three) different electronic transitions from two different lower electronic states, and c) two different energy states of the I atoms. And also the image would be complicated because of a combination of various dissociation processes shown by Reactions 14—17. The anisotropic image of CH_3^+ in the upper left panel of Fig. 1, however, suggests that a) the dissociation path is not predissociative but prompt, and b) the energy distribution is not complicated but simple as proposed by Reaction 7. Thus, it is unlikely for Reactions 14 and 15 to occur.

Reactions 14 and 15 need, in any case, at least four 266 nm photons. Danon et al.[10] found a second or lower order intensity dependence for the I^+ formation, and proposed that formation of I^+ from the photodissociation of CH_3I^+ at 266 nm is less probable than the multiphoton ionization of the photofragments. Since the ionization step of I atoms is easily saturated with a moderate ionization cross section for Reaction 9 and 10, it is reasonable to assume that the photofragment ions observed in this experiment are not produced via Reactions 14 and 15, but rather via multiphoton

ionization of the photofragments after one-photon dissociation of CH_3I molecules.

B. Formation of Fast Methyl Radicals and Slow I Atoms from Photodissociation of Dimers at 266 nm. When a molecular beam of neat CH_3I is supersonically expanded, the clustering is mainly due to dimers and other small clusters. This observation is in accordance with the fact that Syage et al.[3] found a decreasing cluster size distribution in the CH_3I molecular beam. Waschewsky et al.[24] reported that the dimer proportion in a bulb condition of 1.3×10^4 Pa and 200 K is 43—86%. Semiempirical calculations predict a bent head-to-head ground-state equilibrium structure for the dimer, CH_3I–ICH_3.[4] The dissociation energy of the dimer is as large as 500 cm^{-1}.[5] Assuming Reactions 3—5, dissociation of a valence excited CH_3I partner in the dimer results in an intra-cluster collision of the I atom and a collisionless escape of the CH_3 fragment. This reaction scheme is in agreement with our experimental observations that a) slow I atoms have an isotropic central feature in the image, and b) fast CH_3 radicals have an anisotropic ring feature. The nascent I atom from the CH_3I partner is decelerated by intra-cluster collision via Reaction 4 and is scattered isotropically in space. Ogorzalek Loo et al.[16] and Penn et al.[17] observed that cluster formation broadened the time-of-flight spectrum of the photofragment I atoms due to intra-cluster collisions.

Our experimental conditions, which favor dimer formation, yield sharp CH_3^+ ring images at velocities slightly slower than expected for monomer dissociation. The β values of the CH_3 products from the dimers are the same as those from free CH_3I molecules, which suggests that the CH_3 group in the CH_3I dimer points outward and has a collisionless anisotropic angle-velocity distribution, as shown schematically in Reaction 3.

Photodissociation of free CH_3I at 266 nm yields mainly $I(^2P_{1/2})$ and additionally $I(^2P_{3/2})$, with most of the excess energy released into CH_3 radical translation. Comparing the translational energy distributions of CH_3 from the monomer and dimer photodissociation, the *nascent* product ratios, $I(^2P_{1/2})/I(^2P_{3/2})$, are estimated to be almost the same. These results suggest that the dimer dissociation mechanism for CH_3 formation is quite similar to that operative in free CH_3I (n,σ^*) dissociation. It was reported by Donaldson et al.[5] that dimer formation causes only a 500—1000 cm^{-1} blue shift in the A band absorption of the CH_3I moiety due to stabilization of the ground state dimers by a dipole–dipole interaction and not in the valence excited state. Knowing the absorption band of a mixture of monomer and dimer at various mixing ratios, Waschewsky et al.[24] concluded that the dimer has almost the same absorption as the monomer A band in the region $\lambda \leq 300$ nm. Thus, perturbation of the valence excited (n,σ^*) state in the dimer is quite small.

Syage[6] reported, however, that the spin-orbit state distribution of the *final product* I atoms is greatly relaxed in the cluster photodissociation at 266 nm. The ratio of $I(^2P_{1/2})/I(^2P_{3/2})$ was reduced from 2.8 for the monomer to 1.3 for the cluster (mostly dimer) due to an intra-cluster quenching process, that is, an inelastic collision by E → V transfer in the exit channel of Reaction 5. Although our detection of I atoms is not state-selective, it is safe to state that the major central image of I^+ reflects this large contribution of $I(^2P_{3/2})$ products. The quenching of $I(^2P_{1/2})$ by alkyl iodides is primarily physical, and the efficiency is less than 10^{-2} in bulb conditions, where the interaction between $I(^2P_{1/2})$ and alkyl iodides works inefficiently.[25] In the dimer condition, however, the photofragment I atom first approaches the I atom in another CH_3I, and then recoils in the opposite direction. According to Zhong et al.[2] the lifetime of a long-lived complex $[CH_3I\text{–}I]^{\#}$ trapped in the potential well is 1.7 ps. In this long-lived trapped state a nonadiabatic transition from $I(^2P_{1/2})$ to $I(^2P_{3/2})$ is greatly increased.

C. Formation of Fast Iodine Atoms from Photodissociation of Small Clusters at 266 nm. Formation of fast I atoms from cluster dissociation was reported for photodissociation of $(CH_3I)_n$ and $(HI)_n$ by Syage[6] and Young,[18] respectively. Since I_2 is simultaneously formed from the clusters via Reaction 6, sequential photodissociation of this I_2 was proposed to explain formation of the fast I atoms as a probable mechanism.[6] Actually, the $I_2(C\ 1_u)$ state is the upper state of a weak continuum absorption in the region of 230—330 nm with a maximum near 270 nm. One-photon dissociation of I_2 at 266 nm was reported by Clear and Wilson.[26] Dissociation yielded $I(^2P_{3/2})$ and $I(^2P_{1/2})$ with an anisotropy parameter of perpendicular character, $\beta \approx -1$. In contrast, we have measured $\beta \approx 2$ for the fast moving I atoms. Moreover, the fragment translational energy of 16 and 25 kcal mol^{-1} is too small for the photodissociation process of I_2 at 266 nm.

Another possible pathway that involves I_2 is three-photon ionization and fragmentation to yield $I^+(^3P_j)$. This mechanism would release maximum translational energies of 46, 28, and 7 kcal mol^{-1} for $I^+(^3P_j, j = 2,1,0)$ if a portion of the excess energy removed by the photoelectron is neglected. However, the 48 kcal mol^{-1} component did not appear in our experiment. De Vries et al.[27] used time-of-flight spectroscopy to probe the fragments from multiphoton excitation of I_2, observing several processes that yield I^+. They also identified dissociative ionization pathways originating from highly excited Rydberg states of the neutral I_2 to repulsive I_2^+ states. Since I_2 has many accessible states in the ultraviolet and vacuum ultraviolet region, I_2 can absorb many photons to generate several electronically excited states via multiphoton absorption processes.[28] These states may produce neutral I atoms that are easily ionized to I^+ at 266 nm. Thus, this type of multiphoton process would yield I^+ ions that have various different kinetic energies. In contrast, our results show only two sharp ring images. Thus, it is unlikely that the I^+ image comes from the photodissociation of the product I_2 molecules at 266 nm.

Since the dimer dissociation produces only slow I atoms, the most probable pathway for formation of the fast I atom is the dissociation of higher clusters, from which an I atom points outward and should, therefore, have a collisionless anisotropic angle-velocity distribution. Because the anisotropy parameters of the I atoms ($\beta \approx 2$) are the same

as that for the monomer (Fig. 6), the electronically excited CH_3I (n,σ^*) is not perturbed even in these cluster conditions. Thus, our bimodal ring images of the I atoms correspond to formation of $I(^2P_{1/2})$ and $I(^2P_{3/2})$. The present branching ratio of $I(^2P_{1/2})/I(^2P_{3/2}) = 3$ is almost the same as for the monomer,

$$(CH_3I)_nH_3CI + h\nu \longrightarrow (CH_3I)_nH_3C + I(^2P_{1/2})/I(^2P_{3/2}), \quad (18)$$

where $(CH_3I)_n$ stands for a small cluster, and the most probable candidate is a dimer ($n = 2$) with the I–I moiety and a hydrogen bond between the H_3CI partner of Reaction 18. The fast I atom can be generated from the monomer-type photodissociation of H_3CI. Since this I atom does not collide in the cluster, the branching ratio of $I(^2P_{1/2})/I(^2P_{3/2})$ is the same as that from free CH_3I.

Conclusion

Photofragment iodine atoms and methyl radicals from the photodissociation of methyl iodide clusters at 266 nm were detected using ion photofragment imaging spectroscopy. The main feature of the translational energy and angular distributions of the fragments are explained, assuming photodissociation of dimers. A small contribution of the higher clusters is observed in two sharp ring images of I atoms. Based on the discussion about the angular anisotropy parameters, translational energy distributions, and the fragment branching ratio for $I(^2P_j, j = 1/2$ and $3/2)$, it is concluded that the CH_3I chromophore excited to the (n,σ^*) state survives intact within the dimer and higher clusters.

This work was supported by the Japan Society for Promotion of Science, the SECOM foundation, and the Ministry of Education, Science, Sports and Culture.

References

1) A. D. Hammerich, U. Manthe, R. Kosloff, H-D. Meyer, and L. S. Cederbaum, *J. Chem. Phys.*, **101**, 5623 (1994), and references therein.

2) D. P. Zhong, P. Y. Cheng, and A. H. Zewail, *J. Chem. Phys.*, **105**, 7864 (1996); D. P. Zhong and A. H. Zewail, *J. Phys. Chem.*, **A102**, 4031 (1998), and references therein.

3) J. A. Syage and J. Steadman, *J. Chem. Phys. Lett.*, **166**, 159 (1990); J. A. Syage, *J. Chem. Phys.*, **92**, 1804 (1990).

4) P. G. Wang, Y. P. Zhang, C. J. Ruggles, and L. D. Ziegler, *J. Chem. Phys.*, **92**, 2806 (1990).

5) D. J. Donaldson, V. Vaida, and R. J. Naaman, *Chem. Phys.*, **87**, 2522 (1987).

6) J. A. Syage, *Chem. Phys. Lett.*, **245**, 605 (1995).

7) Y. B. Fan, K. L. Randall, and D. J. Donaldson, *J. Chem. Phys.*, **98**, 4700 (1993).

8) D. W. Chandler and P. L. Houston, *J. Chem. Phys.*, **87**, 1445 (1987).

9) Y. Sato, Y. Matsumi, M. Kawasaki, K. Tsukiyama, and R. Bersohn, *J. Phys. Chem.*, **99**, 16307 (1995).

10) J. Danon, H. Zacharias, and K. H. Welge, *J. Chem. Phys.*, **76**, 2399 (1982).

11) T. F. Budinger and G. T. Gullberg, *IEEE. Trans. Nucl. Sci.*, **NS-21**, 2 (1974).

12) D. W. Chandler, J. W. Thoman, M. H. M. Janssen, and D. H. Parker, *Chem. Phys. Lett.*, **156**, 151 (1989).

13) R. K. Sparks, K. Shobatake, L. R. Carlson, and Y. T. Lee, *J. Chem. Phys.*, **75**, 3838 (1981).

14) R. N. Zare and D. R. Herschbach, *Proc. IEEE*, **21**, 913 (1963).

15) M. K. Dzvonik, S-C. Yang, and R. Bersohn, *J. Phys. Chem.*, **61**, 4408 (1974).

16) R. Ogorzalek Loo, G. E. Hall, H-P. Haerri, and P. L. Houston, *J. Phys. Chem.*, **92**, 5 (1988).

17) S. M. Penn, K. J. Hayden, L. R. Carlson, K. J. Muyskens, and F. F. Crim, *J. Chem. Phys.*, **89**, 2909 (1988).

18) M. A. Young, *Chem. Phys.*, **102**, 7925 (1995).

19) T. G. DiGuiseppe, J. W. Hudgens, and M. C. Lin, *J. Chem. Phys.*, **76**, 3337 (1982).

20) D. M. Lubman, R. Naaman, and R. N. Zare, *J. Chem. Phys.*, **72**, 3034 (1980).

21) C. E. Moore, "Atomic Energy Levels," NSRDS-NBS 35, Nat. Bur. Standard, U.S., Washington (1971), Vol. 3.

22) M. Kawasaki, H. Sato, T. Kikuchi, S. Kobayashi, and T. Arikawa, *J. Chem. Phys.*, **87**, 5739 (1987).

23) J. H. Eland, "Electron Spectroscopy; Theory, Techniques and Applications," ed by C. R. Brundle and A. D. Baker, North Holland, Amsterdam (1979), Vol. 3, p. 231.

24) G. C. G. Waschewsky, R. Horansky, and V. Vaida, *J. Phys. Chem.*, **100**, 11559 (1996).

25) R. J. Donovan, F. G. M. Hathorn, and D. J. Husain, *J. Chem. Soc., Faraday Trans.*, **64**, 3192 (1968).

26) R. D. Clear and K. R. Wilson, *J. Mol. Spectrosc.*, **47**, 399 (1973).

27) M. S. De Vries, N. J. A. Van Veen, T. Baller, and A. E. De Vries, *Chem. Phys.*, **56**, 157 (1981).

28) M. Kawasaki, K. Tsukiyama, M. Kuwata, and I. Tanaka, *Chem. Phys. Lett.*, **67**, 365 (1979).